Neural Mass Model of multisensory integration in the Superior Parietal Lobe using intracranial EEG

Article · January 2006

READS
24

4 authors:

Rosalyn J Moran
Virginia Polytechnic Institute and State Uni…
42 PUBLICATIONS **2,267** CITATIONS
SEE PROFILE

Richard B Reilly
Trinity College Dublin
394 PUBLICATIONS **4,131** CITATIONS
SEE PROFILE

Sophie Molholm
Albert Einstein College of Medicine
97 PUBLICATIONS **3,543** CITATIONS
SEE PROFILE

John J Foxe
University of Rochester
314 PUBLICATIONS **13,844** CITATIONS
SEE PROFILE

European Journal of Neuroscience, Vol. 27, pp. 2303–2312, 2008 doi:10.1111/j.1460-9568.2008.06187.x

Changes in effective connectivity of human superior parietal lobule under multisensory and unisensory stimulation

R. J. Moran,[1] S. Molholm,[2,3] R. B. Reilly[1] and J. J. Foxe[2,3]
[1]The School of Electrical, Electronic and Mechanical Engineering, University College Dublin, Dublin, Ireland
[2]Cognitive Neurophysiology Laboratory, Program in Cognitive Neuroscience and Schizophrenia, Nathan S. Kline Institute for Psychiatric Research, Orangeburg, NY 10962, USA
[3]Program in Cognitive Neuroscience, Department of Psychology, The City College of the City University of New York, 138th Street and Convent Avenue, New York, NY 10031, USA

Keywords: effective connectivity, multisensory integration, neural mass models, superior parietal lobule

Abstract

Previous event-related potential (ERP) studies have identified the superior parietal lobule (SPL) as actively multisensory. This study compares effective, or contextually active, connections to this region under unisensory and multisensory conditions. Effective connectivity, the influence of one brain region over another, during unisensory visual, unisensory auditory and multisensory audiovisual stimulation was investigated. ERPs were recorded from subdural electrodes placed over the parietal lobe of three patients while they conducted a rapid reaction-time task. A generative model of interacting neuronal ensembles for ERPs was inverted in a scheme allowing investigation of the connections from and to the SPL, a multisensory processing area. Important features of the ensemble model include inhibitory and excitatory feedback connections to pyramidal cells and extrinsic input to the stellate cell pool, with extrinsic forward and backward connections delineated by laminar connection differences between ensembles. The framework embeds the SPL in a plausible connection of distinct neuronal ensembles mirroring the integrated brain regions involved in the response task. Bayesian model comparison was used to test competing feed-forward and feed-backward models of how the electrophysiological data were generated. Comparisons were performed between multisensory and unisensory data. Findings from three patients show differences in summed unisensory and multisensory ERPs that can be accounted for by a mediation of both forward and backward connections to the SPL. In particular, a negative gain in all forward and backward connections to the SPL from other regions was observed during the period of multisensory integration, while a positive gain was observed for forward projections that arise from the SPL.

Introduction

Functional neuroimaging and electrophysiological techniques have been widely applied in the area of multisensory research to examine the distributed cortical networks responsible for multisensory processing (e.g. Calvert *et al*., 2000; Foxe *et al*., 2000, 2002; Raij *et al*., 2000; Molholm *et al*., 2002, 2004; Laurienti *et al*., 2005). While substantial progress has been made in defining these circuits and in assessing the temporal course of activation across the nodes within these circuits, the key to understanding how multisensory computations are made lies in understanding how the nodes of these circuits interact and the causal relationships between them. The study of effective connectivity based on model-led approaches that make use of the various available classes of neurophysiological data [e.g. functional magnetic resonance imaging (fMRI), electroencephalogram (EEG) and event-related potentials (ERPs)] is one prominent approach to this fundamental issue that has recently been applied (e.g. Pleger *et al*., 2006; Mechelli *et al*., 2003; Bitan *et al*., 2005). These investigations are based on the premise that effective connections display task-dependent activity and mediate processing across all areas active in a given system. Such dynamic causal models, where the EEG, fMRI or ERP time series is represented in an input-state-output sense, make inferences about the system state based on nonlinear generative models that are biologically plausible (see Friston *et al*., 2003; Penny *et al*., 2004; David *et al*., 2006; Stephan *et al*., 2007). The advantage of these so-called 'neural mass models' for ERP data is that both extrinsic and intrinsic anatomic connections, those between and within cortical regions, can be parameterized explicitly. This allows investigation of which components of the dynamics are due to local within-region effects and which arise from longer-range interactions across the nodes of a given network (Kiebel *et al*., 2007; Moran *et al*., 2007). Additionally, application of these models allows for the assessment of the direction of information flow between regions and an estimation of the influence of feedforward and feedback connectivity on processing. In fact, where competing hypotheses exist regarding feedforward or feedback influences on sensory processing, different extrinsic white-matter axonal connections can be embedded in the model and tested using real physiological data (e.g. Garrido *et al*., 2007).

Our goal in this report was to apply neural mass modelling to multisensory data as a means of assessing the contribution of feedforward and feedback processes to ongoing sensory integration processes within an identified node of the audiovisual multisensory

Correspondence: Dr Rosalyn Moran, as above.
E-mail: r.moran@fil.ion.ucl.ac.uk

Received 10 August 2007, revised 28 February 2008, accepted 2 March 2008

processing network, namely the superior parietal lobule (SPL). Multisensory integration refers to the neural integration of inputs from more than a single sense to form unified or unitary multisensory percepts. Typically, cortical and subcortical regions responsible for multisensory integration are identified by assessing the differences in their response properties under unisensory and multisensory stimulation conditions where nonlinear properties are taken to indicate sensory integration. For example, as in the present study, subjects are stimulated with auditory-alone (A), visual-alone (V) and simultaneous auditory-visual (AV) bisensory inputs, and the summed unisensory responses (A + V) are compared to the bisensory response (AV). As voltage sums linearly, any difference between the A + V and AV responses is direct evidence of an interaction (e.g. Giard & Peronnet, 1999; Foxe *et al.*, 2000). The same approach is often taken with haemodynamic imaging data even though linearity cannot be assumed for the blood oxygen level-dependent (BOLD) response (see Laurienti *et al.*, 2005).

Current findings in multisensory integration research support both feedback and feedforward mechanisms. Feedback modulation is characterized by the control of unisensory input by higher cognitive functions such as attention. For example, increased performance in behavioural tasks might be attributed to heightened attention to a given sensory modality due to coactivation of another (e.g. Macaluso *et al.*, 2000; McDonald *et al.*, 2000) or, alternatively, selective attention to one sensory modality might result in suppression of inputs from competing sensory inputs (e.g. Foxe *et al.*, 1998, 2005; Fu *et al.*, 2001; Weissman *et al.*, 2004; Foxe & Simpson, 2005). In such cases, the control of sensory processing, and to some extent of multisensory integration, is thought to be driven by higher-level cortical regions such as the superior temporal sulcus, the inferior parietal sulcus, regions of frontal cortex, the insula and claustrum (e.g. Calvert, 2001; Calvert *et al.*, 2001; Ongur & Price, 2000). Additionally, it was long believed that inputs to the different sensory systems were initially analysed in isolation during passage through the multiple stages of their respective unisensory processing streams before integration occurred in higher-order 'multisensory' regions of the cortex. Under this view, multisensory interactions that were found at early cortical processing stages, stages that had traditionally been thought of as strictly 'unisensory', were assumed to reflect feedback modulations that proceeded from multisensory processing in the higher-order multisensory areas. However, it is now widely accepted that strict sensory segregation does not pertain during the earliest phases of cortical processing and that there is substantial feedforward convergence and integration in early 'unisensory' processing regions (see Schroeder & Foxe, 2002, 2005; Foxe & Schroeder, 2005). Thus, the mode of operation of any given node in the multisensory processing network might rely on either or both mechanisms.

Neural mass models of cortical neurons offer valuable insight into the generation of the EEG and underlying local field potentials (Lopes da Silva *et al.*, 1974; Wendling *et al.*, 2000). One particular neural mass model, which is based on a biologically plausible parameterization of the dynamic behaviour of the layered neocortex, has been successfully used to generate signals akin to those observed experimentally, including small-signal harmonic components such as the alpha band and larger, transient, ERPs (Jansen & Rit, 1995). The goal of neural mass modelling is to understand the neuronal architectures that generate electrophysiological data, where key model parameters are sought to explain observed changes in EEG output. In the present study we took advantage of a unique intracranial dataset where highly consistent multisensory audiovisual interactions were recorded directly from the SPL of three human epilepsy patients performing a simple reaction-time task (Molholm *et al.*, 2006). We used this dataset to model the unisensory-auditory and unisensory-visual component pathways using a data-driven approach and then compared simulated multisensory outputs to actual recorded multisensory ERPs from the SPL. The approach we followed used the unisensory ERP data (A and V) to construct the most plausible network that could generate the multisensory ERP response in the SPL. We did this by modelling the unisensory data first. We then had a 'baseline' value for the active connections to and from the SPL under auditory-alone stimulation and a 'baseline' value for the active connections under visual-alone stimulation. The most basic AV network is assumed to take the form of a simple linear sum of unisensory connection strengths (A + V). Any changes from this basic AV = A + V network is assumed to underlie the key 'integration'. This is the very definition of an integration effect in neuroimaging studies. We tested for changes from this A + V baseline by using the real multisensory ERP data. Model inversion uses the Bayes principle, which specifies priors on the parameter values. These priors are taken as the basic A + V. If no change from this basic condition occurred during multisensory integration then the inversion scheme would similarly result in no change in parameters from its priors values. We then tested three possible modulations to this network that can generate the real measured multisensory (AV) ERP. These three models comprise (i) changes in feedforward connections only, (ii) changes in feedback connections only and (iii) changes in both feedforward and feedback connections. Bayesian model comparison was used to estimate which of the three is most likely to account for the data. Differences in the extrinsic connections to the SPL were studied to investigate how the perceptual system changes form to affect multisensory integration.

Materials and methods

Modelling approaches for ERP investigation

Neural mass models of the EEG originated with Wilson & Cowan (1973), who theorized that on a scale greater than a few millimeters, the dynamics of large interacting groups of neurons could be described by a few average population variables. A cortical area, understood as an 'ensemble' of strongly interacting macro-columns of granular and agranular cells, has been modelled in a dynamic framework by Jansen and Rit (for its formal mathematical description see Jansen & Rit, 1995). They provided parameter values for the different cell proportions and synaptic responses based on *in vitro* animal anatomical investigations. Their model produced similar timing and amplitude effects to human visual evoked potentials, and also demonstrated that the ensemble could produce characteristic alpha wave activity. The ensemble contains pyramidal, inhibitory and granular stellate excitatory cells and the EEG is assumed to be generated by the synchronous dendritic activity of the pyramidal cell group (Steinschneider *et al.*, 1992; Niedermeyer & Lopes da Silva, 2004).

The hierarchical arrangement of sensory cortices has been delineated on the basis of laminar connections among different cortical areas. Based on neuroanatomic studies of the monkey visual cortex, Felleman and Van Essen (1991) provide a tri-partitioning of the cortical sheet into supra- and infra-granular layers and granular layer IV, which have certain extrinsic connections (those that traverse white matter and connect cortical regions and subcortical structures). Three kinds of interarea connectivity were described and these have been incorporated by David *et al.* (2006) into the single-mass model in order to examine the effects of feedforward and feedback connections on ERP generation. These are described by heterogeneous and highly asymmetric coupling among the different layers of interacting neural masses. These are (i) forward connections that originate in supra-

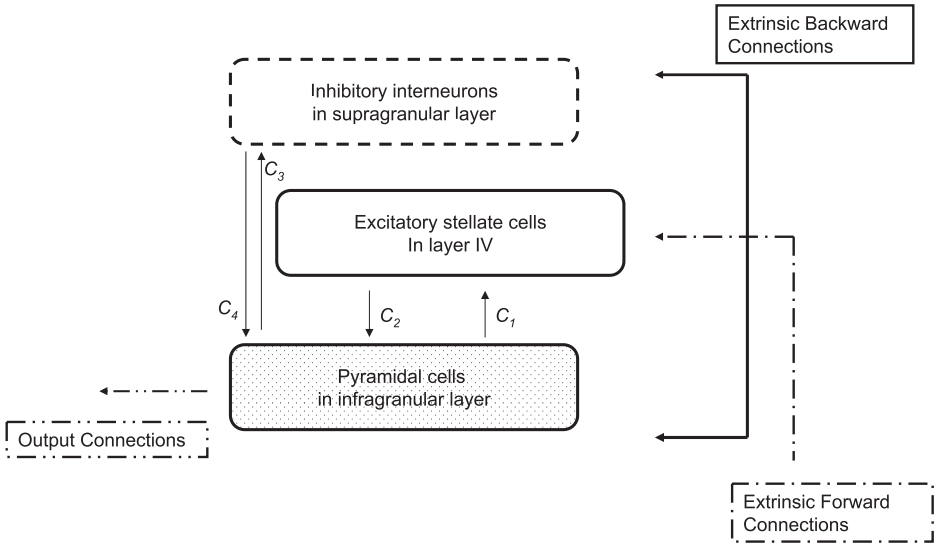

FIG. 1. SPL Cortical sheet receiving extrinsic input to different cell types, characterizing feedforward, feedback and lateral connections. Pyramidal cells and inhibitory interneurons are found in both infra- and supragranular layers in the cortex, and granular excitatory cells are found in layer IV. The assignment of neuronal populations to layers is important for multiarea models with connections that reflect the hierarchical position of the areas and have layer-specific terminations (adapted from David *et al*., 2006).

granular and infra-granular layers and terminate in layer 1V, (ii) backward connections where only supra- and infra-granular layers are connected, and (iii) lateral connections that originate in both supra- and infra-granular layers and target all layers (see Fig. 1). The model has been used previously for human scalp EEG data to examine connectivity changes to the network subtending category-specific visual processing, with model connection changes validated using functional magnetic resonance imaging (David *et al*., 2006). Recently, in a study by Garrido *et al*. (2007), competing models of the kind used here demonstrated reproducible connectivity changes across subjects during oddball responses in a mismatch negativity paradigm. The study by Garrido *et al*. (2007) also used scalp EEG.

The data acquired for our study comprised intracortical EEG. This means that the whole network involved in multisensory processing could not be examined. However, as the terminations of feedforward and feedback connections to a certain area (here the SPL) are asymmetrical and heterogenous, we can examine their separate effects in parallel.

The following exposition of this type of hierarchical framework, in the context of multisensory ERPs, should uncover where feedback or feedforward effects are most salient in the perceptual process.

Experimental subjects

Data from three individuals (ages 29, 35, and 45 years) with epilepsy were used. The basic ERP effects were reported previously (Molholm *et al*., 2006). The patients (referred to as D.M., K.K. and V.H. throughout) were implanted with subdural electrodes for evaluation of the foci of pharmacologically intractable epilepsy. They were all males and two were right-handed. Recordings were made after all clinical procedures related to seizure localization were completed. During localization procedures, subjects were removed from their antiepileptic medications until sufficient numbers of seizures were recorded but when these clinical measures were completed they were immediately returned to their regular dosages. All recordings for the present study were made after subjects had been re-started on their medications. All subjects provided written informed consent after the procedures were fully explained to them. The Institutional Review Boards at both Nathan S. Kline Institute and at Weill Cornell Medical College approved all experimental procedures, which were in accordance with NIH guidelines.

Stimulation and task

The auditory stimulus was a 1000-Hz tone (60 ms duration, 10 ms rise and fall times; 75 dB SPL) that was presented over headphones. Visual stimulation was comprised of a simple red disk (60 ms duration), subtending 1.2° in diameter (140 cm viewing distance) on a black background. Subjects were instructed to make a rapid button press response whenever a stimulus in either stimulus modality was detected, as quickly as possible. The three stimulus conditions (auditory, visual and bisensory audiovisual) were presented with equal probability in random order. Stimulus onset asynchrony varied randomly between 750 and 3000 ms. Stimuli were delivered in blocks of 150 trials. Frequent breaks were provided to maintain concentration and to prevent fatigue.

EEG recordings

Continuous EEG from 75–118 subdurally placed electrodes was recorded using BrainAmp^{TM} amplifiers (Brain Products GmbH, München, Germany). The data were bandpass-filtered online from 0.05 to 100 Hz and digitized at 1000 Hz. The continuous EEG was divided into epochs from 100 ms before to 250 ms after stimulus onset and baseline-corrected over the full epoch. An artifact criterion of ±300 μV was applied to electrodes within the region of interest to reject trials with excessive noise transients. An average of 350 trials was accepted per stimulus condition. When clean averages had been obtained, baseline was redefined as the epoch from −100 to 0 ms prior to stimulus onset. EEG epochs were sorted according to stimulus condition and averaged for each subject to compute the ERP.

For all subjects, the electrode site from which data were analysed was chosen based on the following criteria: (i) it was over the parietal cortex; (ii) both auditory and visual stimuli elicited a robust unisensory response at the site; and (iii) both the auditory and the visual responses were larger than the corresponding responses from the surrounding electrodes. In two of the subjects the electrode that met the predetermined criteria was located just anterior to the intraparietal sulcus over the superior parietal lobule. In the third subject the location was located on a somewhat more lateral and anterior portion of the parietal lobe. However, the sparser electrode coverage (strips rather than grids were used in this subject) prevented as precise a localization of this activity as was possible for the first two subjects. Nonetheless, the highly similar morphology and timing of the responses to those of the other subjects strongly suggests a similar origin. Figure 2 displays the location of the electrode for each of the subjects. Greater detail regarding electrode localization and the sharp focus of multisensory activity within the SPL is provided in Molholm *et al*. (2006). EEG epochs were sorted according to stimulus condition and averaged for each subject to compute the ERP. Statistics were performed on individual subject data.

Auditory and visual component models

Each neural mass model was parameterized by a system of six state equations (Supplementary material, Appendix S1) describing the population firing rate and postsynaptic potentials within a mass, and feedforward and feedbackward gain parameters impinging on the mass. The parameters of interest are these second gain parameters which model the input to and output from the SPL (Fig. 1); a feedforward population (Region 1), a feedback population (Region 3), feeding to the SPL (Region 2). These parameters of interest, θ, included feedback connections from the SPL to Region 1 [backward connection $(BC)_{1,2}$], feedback connections from Region 3 to the SPL ($BC_{2,3}$), feedforward connections from Region 1 to the SPL [forward connection $(FC)_{2,1}$] and feedforward connections from the SPL to

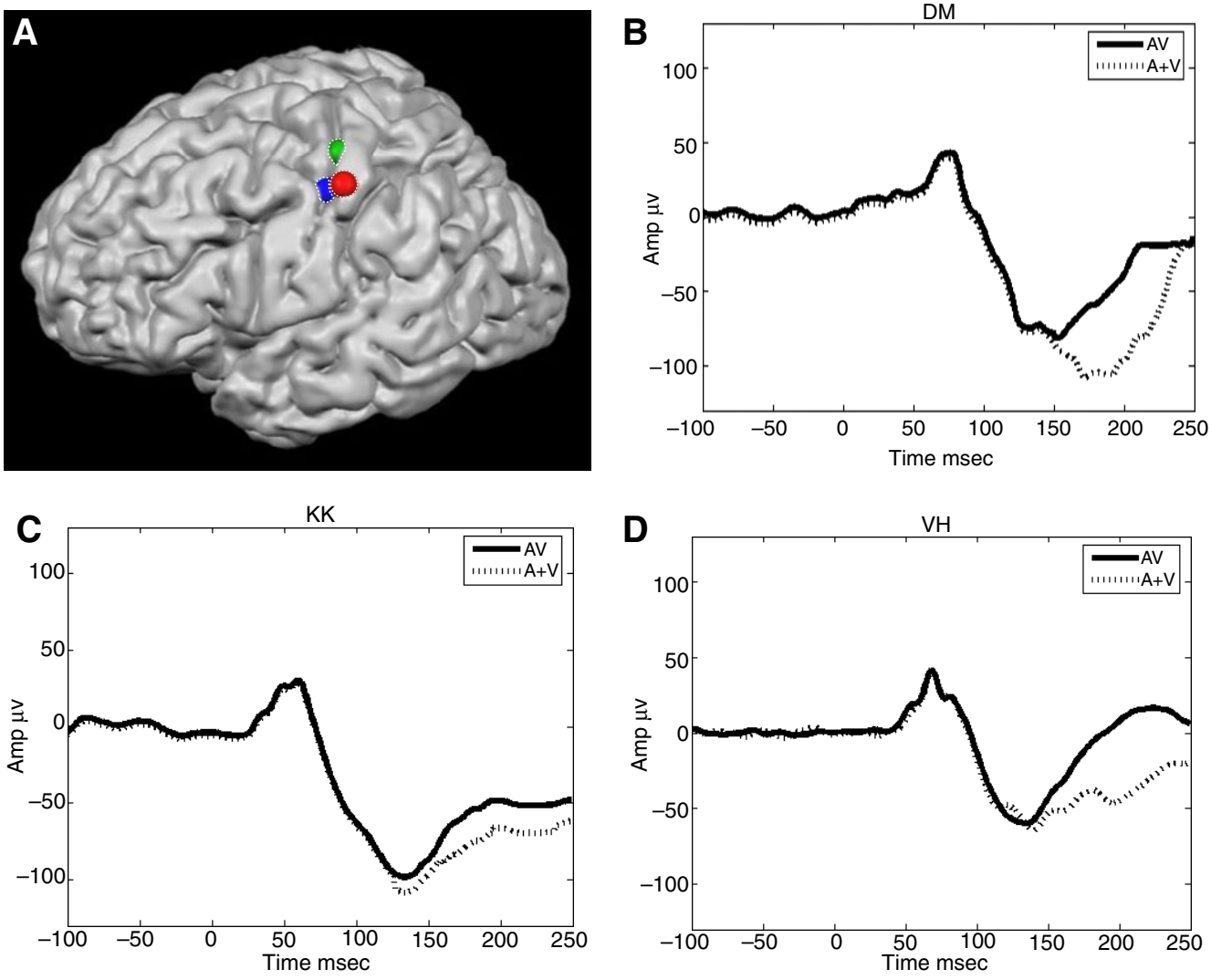

FIG. 2. (A) Superior parietal lobule electrode positions (see dotted white lines) for subjects D.M. (lower right), K.K. (lower left) and V.H. (top). In Talairach coordinates these positions are: D.M., (−52, −18, 50); K.K., (−44, −14, 46); and V.H. (−40, −20, 57). (B–D) Average ERPs for each subject, recorded from the electrodes at the positions given in A. Broken traces illustrate summed audio and visual (A + V) recorded ERPs, thick traces illustrate the recorded audiovisual (AV) ERP.

Region 3 ($FC_{3,2}$). (Note the use of conventional notation where the second subscript sends to first subscript.) The optimization involved maximizing the log model evidence with respect to the connectivity parameters θ from a three-source hierarchy.

The optimization was conducted using an expectation-maximization routine from the Statistical Parametric Mapping (SPM) software package (SPM5; Wellcome Trust Centre for Neuroimaging, London, UK, http://www.fil-.ion.ucl.ac.uk/spm). SPM for dynamic causal models of magnetoencephalogram (MEG) and EEG event-related responses (Kiebel & Friston, 2004; David *et al*., 2006) is intended for use on high-density scalp EEG and MEG data. The lead field of this work (mapping source space to sensor space) was not necessary here as, in the model, the (dendritic) membrane potential of pyramidal cells provides the cortical output as measured with the local field potential. This is based on the fact that the apical dendrites of these cells orientate perpendicularly to the cortical surface providing maximally congruent postsynaptic potentials (Nunez & Srinivasan, 2006; Schwartz *et al*., 2006). The estimation scheme was originally introduced for dynamic causal models of functional imaging data (Friston *et al*., 2003; Penny *et al*., 2004) where the moments of the posterior distribution of connection parameters are estimated using the Bayes rule (Kass & Raftery, 1995). The posterior moments, $q(\theta)$ are updated iteratively using Variational Bayes where the moments of the parameters to be optimized are assumed to be Gaussian in their probability distribution and to independently impact the ERP output. Optimization involves a gradient ascent on the free energy (F) of the system, parameterized by the parameter set θ representing the extrinsic connections and measurement noise with covariance λ. This free energy approximates the log evidence and can be decomposed into two components (described below): an accuracy term, which quantifies the data fit, and a complexity term, which penalizes models with a large number of parameters. Therefore, the evidence prevents artificial result enhancements from an 'overfitting' model with more free parameters. The prior variance of intrinsic parameters was set to zero, allowing changes in only extrinsic connectivity between the three populations. The fixed intrinsic parameters were set at standard SPM for ERP values, derived from the anatomical studies of Jansen & Rit (1995; see also Table 1). Thus the final *a posteriori* estimates for these connection parameters can be assessed in terms of competing model structure. Below we test three suitable candidate models.

Repeat until convergence:

$$\text{E-step} \quad \theta_{i+1} \rightarrow \max|_{\theta_i} F(\theta, \lambda) \text{ and}$$

$$\text{M-step} \quad \lambda_{i+1} \rightarrow \max|_{\lambda_i} F(\theta, \lambda) \text{ where} \qquad (1)$$

$$F(\theta, \lambda) = \langle \ln(y|\theta, \lambda) + \ln q(\theta) - \ln p(\theta) \rangle \qquad (2)$$

The prior assumptions about the connectivity parameters are given by $p(\theta)$. In simulations, the parameter values are assigned log-normal priors with large variance. The log normal initial values are exponentially transformed to ensure positivity, a natural physical constraint. For forward connections density $\xi_i \sim N(0, C_\xi)$, the state equations use $\theta_i = \mu_i \exp(\xi_i)$ with $\mu_i = 350$, and for the backward connections $\mu_i = 50$. The variance of the initial estimates, C_ξ, is 0.5, corresponding to a relatively uninformed initial value that allows scaling up to an order of magnitude in the posterior density.

Optimization was performed on an approximation to the conditional (posterior) density, using the iterative estimates of the likelihood probability. Optimization was performed for each subject's grand averaged auditory (A) and visual (V) response from stimulus onset to 250 ms post-stimulus. The inputs consisted of delta functions to the feedforward population (population 1; see Fig. 3). This was sized as per the original ERP study by Jansen and Rit to produce sufficient excitation for an ERP to emerge over simulated background noise (Jansen & Rit, 1995). The unitary, A and V maximum *a posteriori* (MAP) estimates for connection parameters then served as initial parameter values in the AV condition. Hence multisensory integration can be formally described as a difference between a combination (linear sum) of the A and V response ERPs and the measured AV ERP., i.e. one may test specifically what connectivity changes most probably occur in the AV condition compared to the A + V condition during the integration effect. This difference serves as the definition of an integration effect in ERP studies (Foxe *et al*., 2000). The MAP estimates for the A and V connections were summed linearly for the initial values on AV and so represent a linear stimulus summation starting point. The AV response was then constructed from a three-layer hierarchy using the same estimation-maximization (E-M) scheme.

Bayesian model selection provides a method for evaluating different types of models (see Eqn 6 of Raftery, 1995; Penny *et al*., 2004).

TABLE 1. Model parameters for each cortical pool

Parameter	Description	Value
Synapse linear impulse response		
Excitatory		
H_e	Maximum amplitude of the excitatory postsynaptic potential	4 mV
τ_e	Time constant of passive membrane and spatially distributed delays in the dendritic tree excitatory population	8 ms
Inhibitory		
H_i	Maximum amplitude of the inhibitory postsynaptic potential	32 mV
τ_I	Time constant of passive membrane and spatially distributed delays in the dendritic tree: inhibitory population	16 ms
Wave to pulse sigmoidal transfer function		
e_0	Maximum firing rate of the neural population	2.5 s^{-1}
v_0	The PSP for which a 50% firing rate is achieved	6 mV
r	Sigmoid linear slope approximation	0.56 mV^{-1}
Intrinsic synaptic connectivity constants		
C_1	Proportional to the number of synapses made by the pyramidal neurons to the dendrites of the excitatory stellate loop	128
C_2	Proportional to the number of synapses made by the excitatory stellates to the dendrites of pyramidal cells	102
C_3	Proportional to the number of synapses made by the pyramidal cells to the dendrites of the inhibitory interneurons	32
C_4	Proportional to the number of synapses made by the inhibitory interneurons to the dendrites of pyramidal cell group	32

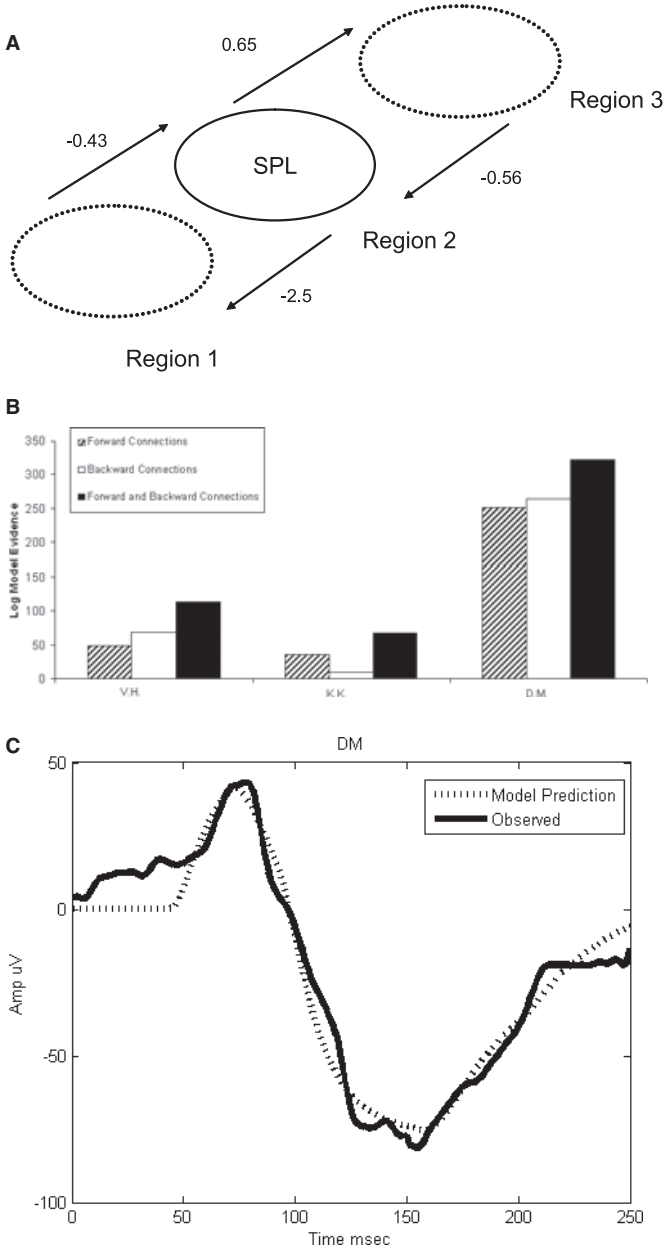

FIG. 3. (A) Schematic of the dynamic causal model used to make inferences about changes in connectivity for multisensory vs. unisensory conditions. Ellipses represent three different populations of neurons. The hatched ellipses represent areas upstream (Region 1) and downstream (Region 3) of the SPL (Region 2); respectively, they send feedforward projections to and receive feedforward projections from the SPL. These areas are also connected via feedback connections that differ from feedforward connections in terms of their laminar termination profile. Backward connections are shown as hashed lines and forward connections are shown as full lines. Beside each connection the average gain in connection strengths for multisensory relative to summed unisensory models is shown. (B) The bar graphs present model evidence for the AV model that allowed (i) changes in forward connections only (blue bars), (ii) changes in backward connections only (green bars) and (iii) changes in forward and backward connections (red bars). The Bayes factor for the best-performing relative to the next best-performing model is shown beside the bars. It can be seen that the scheme strongly favours the mixed forward-and-backward model. (C) An example of the best-performing ERP model fit (i.e. the mixed forward-and-backward model) for subject D.M.'s recorded data (bisensory AV condition) is illustrated.

Using the output of the variational E-M objective function one can calculate the model evidence and compare what type of model best captures that data's structure. Before conducting an analysis of AV MAP connection estimates, three types of models (dynamic causal models) were compared. The first model allowed changes in forward connection only between the A + V and the AV condition, the second model allowed changes in backward connections only and the third model allowed changes in both forward and backward connections.

Model evidence:

$$p(y|m) = \int p(y|\theta m)p(\theta|m)d\theta \quad (3)$$

Atthe final M-step, the free energy value gives the log model evidence ln $p(y|\lambda m) \approx \ln p(y|m)$. The term consists of model accuracy and complexity, penalizing more complex models when similar accuracies exist.

Log model evidence:

$$\ln p(y|m) = Accuracy(m) - \text{Complexity}(m) \quad (4)$$

Theterm thus gives the most likely model candidate for the given data. It is used below to distinguish between three possible sets of posterior parameter (connection) values. The ratio of model evidence for models i and j is given by the Bayes factor B_{ij}. A Bayes factor of 20–150 represents strong evidence in favour model i over model j, and factors >150 represent very strong evidence (see table 1 in Penny *et al.*, 2004 for a full interpretation of these metrics and their comparison to classical P-statistics.)

Results

Behavioural results

Across the three subjects, reaction times were fastest for the multisensory condition (average 279 ms), intermediate for the auditory condition (334 ms) and slowest for the visual condition (355 ms). This pattern of results is equivalent to that observed in an earlier study on a larger sample of 12 subjects (Molholm *et al.*, 2002; see also Murray *et al.*, 2005), in which the differences were found to be statistically significant.

For individual subjects, the pattern of reaction times was for the most part paralleled by accuracy as measured by percentage hits. The individual performance data (reaction-times and percentage hits) are presented in Table 2. This rapid response time is characteristic of multisensory environments where performance is heightened (e.g. Hairson *et al.*, 2003; Zuidpek *et al.*, 2004; Senkowski *et al.*, 2007). The implications of these behavioural data were discussed at length in Molholm *et al.* (2006) and will not be discussed further in the present report.

TABLE 2. Behavioural data: mean reaction times (RT) in ms and percentage hits for each subject for each stimulus condition

	Audiovisual		Auditory		Visual	
Subject	RT (ms)	Hits (%)	RT (ms)	Hits (%)	RT (ms)	Hits (%)
K.K.	359	87	471	72	409	82
V.H.	243	94	270	89	341	91
D.M.	236	91	260	90	314	88

ERP posterior density estimates and model evidence

A posteriori estimates of the connectivity parameters for the auditory-alone and visual-alone unisensory conditions are presented for each subject in Table 3. These are the log-normal probability densities constituting a defining mean and variance per parameter (i.e. the four possible connections to and from SPL: $BC_{1,2}$, $BC_{2,3}$, $FC_{2,1}$ and $FC_{3,2}$). Parameter labels use the second-to-first subscript notation in describing the connectivities. These MAP estimates are summed for each connection to provide the reference AV model. They demonstrate active connections in both the feedforward and feedback directions to the SPL under unisensory stimulation. Using a linear sum of these values as the initial value (baseline) AV parameters we then observed changes when inverting the model using the multisensory ERP. These parameters, as referred to the A + V baseline, are presented in Table 4. Table 5 presents the log model evidence for each three models for each subject, referred to the simple linear A + V model.

The general scheme output is depicted in panel A of Fig. 3 where the data from the SPL are modelled by changes in connectivity patterns into and out of SPL (i.e. Region 2) from 'unknown' sources (Regions 1 and 3, respectively; broken outlines). Unknown sources refer to those cortical regions immediately downstream of SPL in the processing hierarchy [i.e. the cortical region(s) to which SPL projects] and those immediately upstream [i.e. the region(s) that project to SPL]. The log model evidence for the best scheme describing AV data is presented in bar charts in panel B of Fig. 3. Here the log Bayes factor representing the difference between the best and next best performing model is presented, relative to the unchanged A + V (starting) model. These values of Bayes factor provide strong evidence (see Penny *et al*., 2004) in favour of an AV model where the observed integrative ERP effects are generated by a mixture of both feedforward and feedback contributions.

TABLE 3. Subjects' log-normal posterior density estimates for connectivity underlying unimodal responses

	MAP estimates for connectivity underlying unimodal responses		
	V.H.	K.K.	D.M.
Audio			
$FC_{2,1}$	*N*(0.5159,0.0073)	*N*(00.5378,0.0016)	*N*(0.2422,0.0011)
$FC_{3,2}$	*N*(3.356,0.0746)	*N*(02.8937,0.0263)	*N*(0.3219,0.0101)
$BC_{1,2}$	*N*(−2.149,0.4996)	*N*(0.0311,0.5)	*N*(−0.0263,0.4981)
$BC_{2,3}$	*N*(0.517,0.0017)	*N*(0.5916,0.0007)	*N*(0.1798,0.0003)
Visual			
$FC_{2,1}$	*N*(−0.3484,0.0111)	*N*(−0.1380,0.0021)	*N*(0.0420,0.1305)
$FC_{3,2}$	*N*(0.0655,0.0598)	*N*(2.0683,0.0296)	*N*(0.0831,0.0829)
$BC_{1,2}$	*N*(0.0414,0.0298)	*N*(−0.1024,0.4990)	*N*(0.0820,0.2109)
$BC_{2,3}$	*N*(−1.9684,0.0073)	*N*(−0.5897,0.0013)	*N*(0.0978,0.0022)

BC, backward connection; FC, forward connection.

TABLE 4. Subjects' log-normal posterior density estimates for connectivity underlying multisensory responses

	MAP estimates for connectivity underlying multisensory responses		
	V.H.	K.K.	D.M.
$FC_{2,1}$	*N*(−0.439,0.0067)*	*N*(−0.6363,0.0056)*	*N*(−0.218,0.001)*
$FC_{3,2}$	*N*(−1.3967,0.127)*	*N*(1.912,0.052)	*N*(1.43,0.024)
$BC_{1,2}$	*N*(−0.0119,0.3898)*	*N*(−2.303,0.427)*	*N*(−5.09,0.1715)*
$BC_{2,3}$	*N*(−0.5408,0.008)*	*N*(−0.259,0.0012)*	*N*(−0.897,0.0006)*

BC, backward connection; FC, forward connection. *Negative gains.

TABLE 5. Log-model evidence for forward, backward and mixed forward-and-backward models, relative to a simple linear A + V reference

Model evidence	V.H.	K.K.	D.M.
Forward connectivity changes	48	35	251
Backward connectivity changes	69	10	264
Forward-and-backward connectivity changes	113	68	322*

*Most strongly demonstrated model.

Discussion

A major goal of the present study was to demonstrate the utility of the neural mass modelling approach when applied to human intracranial electrophysiological data, and in particular to issues in multisensory integration. The extent to which multisensory integration effects that have been found in human cortex are driven by feedforward or feedback inputs, or indeed by a mixture of both, is a matter of vigorous investigation in the field (see, e.g., Foxe & Schroeder, 2005; Macaluso & Driver, 2005). Here we applied the approach to recordings made directly from the human SPL as subjects performed a simple rapid reaction time task. As with all modelling studies, model inversion accounts for changes in parameters across different data sets; however, they do not account for physiological factors that are not parameterized in a model. For this reason data-driven modelling studies must be hypothesis-driven. The underlying hypothesis in this study is that connection changes account for the majority of data change among unisensory and multisensory conditions. This is interesting, due to the competing theories mentioned above that specifically speak to top-down and bottom-up contributions to multisensory integration and to more theoretical accounts of neuronal organization that describe the role of these connections in permitting contextual and environmental expectations to permit current perception (Rao & Ballard, 1999; Friston, 2005). Clearly other effects within the SPL may be actively changing across conditions and these are not accounted for in the inversion. Other models describing intra-area changes, for example, could give similar model evidence. However, in this study we aimed to answer the question, how do feedback and feedforward network connections affect the SPL during multisensory integration? In this respect the model gave clear answers with formal model comparison lending strong evidence to one model over others.

Clear and highly replicable multisensory integration effects were seen in all three subjects and we applied neural mass modelling to explain the mechanisms driving these effects. A mixed model that comprised both feedforward and feedback influences best approximated the multisensory integration effects seen in SPL. Two other models tested, one that relied exclusively on feedforward connections and a second that relied exclusively on feedback connections, failed to accurately account for the observed physiological data. The mixed model provides an excellent fit for the observed data as demonstrated by the large Bayes factors obtained for this model relative to either of the other tested models (see Raftery, 1995; Penny *et al*., 2004).

While the main thrust of multisensory neuroimaging research in humans to this point has been in mapping the cortical regions that perform multisensory integrative operations, simply localizing these regions does not go far towards explaining what their specific role in integration is. Similarly, while ERPs have provided quite specific information about the relative timing across the nodes of these

multisensory networks, and inferences can thus be made regarding the level of processing engaged in by a given region, the degree of specificity regarding mode of operation is still highly impoverished. This is not the case for invasive studies in nonhuman primates (e.g. Schroeder *et al*., 2001; Lakatos *et al*., 2007) where the use of multicontact translaminar electrodes has allowed for direct testing of the feedforward and feedback nature of multisensory effects based on the observed laminar activation patterns (see Schroeder & Foxe, 2002; Schroeder *et al*., 2004). Of course, similarly invasive studies in humans are not a viable option for most studies of multisensory integration and yet it would be of tremendous utility to be able to infer directionality of information flow and the relative contributions of various input types. Moreover, many of the multisensory functions researchers are particularly interested in, especially multisensory speech comprehension (e.g. Pekkola *et al*., 2006; Ross *et al*., 2007; Saint-Amour *et al*., 2007), high-level attentional interactions (e.g. Eimer & van Velzen, 2005) and issues in human clinical conditions such as schizophrenia (Surguladze *et al*., 2001), are not possible in animal models. As such, the demonstration here that meaningful inferences about the directionality of information flow, based on realistic models of laminar-specific interareal connectivity patterns, can be made from surface-recorded human ERPs, suggests that application of this approach can provide valuable new insights into the operation of distributed cortical processing networks.

One potentially puzzling aspect of the model's best estimate is the observation of negative gain values in connection strength for both feedforward and feedback connections during the integration period. The implication is that some form of sequestration of SPL processing occurs during this period, such that SPL ceases to be influenced as greatly by either its input or output regions. The results suggest that SPL, experiencing a reduction in signal input from other regions, may become isolated for intrinsic processing of audiovisual information. This result provides a testable hypothesis for further investigation.

Previous studies of effective connectivity that have employed neural mass models have, in the main, used scalp-recorded EEG (e.g. Garrido *et al*., 2007; Kiebel *et al*., 2007), with the inherent problem of inaccuracies in generator localization. That is, in order to assess effective connectivity between regions, the scalp-recorded data with its spatial smearing due to volume conduction must first be source-localized. The source localization scheme is an add-on to the neural mass model, requiring further parameters that must be estimated in an inversion scheme (Kiebel *et al*., 2006). The estimation of intracranial generators, the so-called 'inverse problem', is ill-posed and models are difficult to verify and often subject to experimenter bias, especially when equivalent current dipole schemes are employed. Inaccuracies in realistically modelling the resistivity of the various surfaces and coverings of the head and brain (e.g. scalp, skull and cerebrospinal fluid) and in realistically approximating the shape of the volume conductor can also lead to localization errors. Determining the minimum and maximum number of active sources is a particularly vexing problem (see Michel *et al*., 2004 for a comprehensive treatment of these issues). So, while future work could examine scalp EEG and MEG data, which offer the possibility of testing connections across the entire multisensory network, the accuracy of this work would be predicated upon a source localization scheme that accurately describes the output of the individual intracortical generators. This source-localization problem is circumvented in the present study where the output of only a single multisensory region could be assessed in isolation because of our use of intracranial electrodes (see Molholm *et al*., 2006). (In terms of output, the model in its form here only assumes that pyramidal cell dendritic orientations provide local field potential measures in the form of their congruent membrane depolarization.) Of course, while we gain greatly in localization accuracy and, as such, we can model contributions to and from the SPL with confidence, we lose the ability to assess other nodes of the network and can only make inferences about regions directly upstream and downstream. Retrograde tracing studies of the superior parietal cortex of rats and macaques could provide hypothetical routes for our multisensory network. Such information could ameliorate some of these problems associated with a scalp, whole-brain, EEG study. Findings have shown connections directly from areas of the superior temporal sulcus to areas near the SPL (Reep *et al*., 1994; Seltzer & Pandya, 2004). Projections from the SPL have been shown to terminate in premotor areas (Wise *et al*., 1997) which may contains neurons that have been identified as multisensory in single-cell studies (Fogassi *et al*., 1996). However, the quality of data, with mimimal spatial smearing compared to scalp data and a precisely known location, allows the multisensory integration effect to be maximally observed in the ERP.

Supplementary material

The following supplementary material may be found on
http://www.blackwell-synergy.com

Appendix S1. A system of six state equations describing the population firing rate and postsynaptic potentials within a mass, and feedforward and feedbackward gain parameters impinging on the mass.

Please note: Blackwell Publishing are not responsible for the content or functionality of any supplementary materials supplied by the authors. Any queries (other than missing material) should be directed to the correspondence author for the article.

Acknowledgements

This work was supported by US National Institute of Mental Health (NIMH) Grants RO1 MH65350 to J.J.F. and RO3 MH79036 to S.M. R.J.M. is supported by the Irish Research Council for Science Engineering and Technology. Additional support was provided by an Irish Higher Education Authority Grant R9310to R.B.R.

Abbreviations

A+ V, summed unisensory responses; A, auditory-alone; AV, bisensory response; BC, backward connection; EEG, electroencephalogram; ERP, event-related potential; FC, forward connection; MAP, maximum *a posteriori*; MEG, magnetoencephalogram; SPL, superior parietal lobule; V, visual-alone.

References

Bitan, T., Booth, J.R., Choy, J., Burman, D.D., Gitelman, D.R. & Mesulam, M.-M. (2005) Shifts of Effective Connectivity within a Language Network during Rhyming and Spelling. *J. Neurosci*, **25**, 5397–5403.

Calvert, G.A. (2001) Crossmodal processing in the human brain: insights from functional neuroimaging studies. *Cerebral Cortex*, **11**, 1110–1123.

Calvert, G.A., Campbell, R. & Brammer, M.J. (2000) Evidence from functional magnetic resonance imaging of crossmodel binding in the human hetero-modal cortex. *Current Biology*, **10**, 649–657.

Calvert, G.A., Hansen, P.C., Iversen, S.D. & Brammer, M.J. (2001) Detection of audio-visual integartion sites in humans by application of electrophys-iological crieria to the BOLD effect. *Neuroimage*, **14**, 427–438.

David, O., Kiebel, S.J., Harrison, L.M. & Mattout, J. (2006) Dynamic causal modeling of evoked responses in EEG and MEG. *Neuroimage*, **30**, 1255–1272.

Eimer, M. & van Velzen, J. (2005) Spatial tuning of tactile attention modulates visual processing within hemifields: an ERP investigation of crossmodal attention. *Exp. Brain Res.*, **166**, 402–410.

Fellemann, D.J. & Van Essen, D.C. (1991) Distributed hierarchical processing in the primate cerebral cortex. *Cerebral Cortex*, **1**, 1–47.
Fogassi, L *et al.* (1996) Coding of peripersonal space in inferior premotor cortex (area F4). *J. Neurophysiol.*, **76**, 141–157.
Foxe, J.J., Morocz, I.A., Murray, M., Higgins, B.A., Javitt, D.C. & Schroeder, C.E. (2000) Multi-sensory auditory–somatosensory interactions in early cortical processing revealed by high-density electrical mapping. *Cognitive Brain Res.*, **10**, 77–83.
Foxe, J.J. & Schroeder, C.E. (2005) The case for feedforward multisensory convergence during early cortical processing. *Neuroreport*, **16**, 376–392.
Foxe, J.J. & Simpson, G.V. (2005) Biasing the brain's attentional set: II. effects of selective intersensory attentional deployments on subsequent sensory processing. *Exp. Brain Res.*, **166**, 393–401.
Foxe, J.J., Simpson, G.V. & Ahlfors, S.P. (1998) Parieto-occipital approximately 10 Hz activity reflects anticipatory state of visual attention mechanisms. *Neuroreport*, **9**, 3929–3933.
Foxe, J.J., Simpson, G.V., Ahlfors, S.P. & Saron, C.D. (2005) Biasing the brain's attentional set: I. cue driven deployments of intersensory selective attention. *Exp. Brain Res.*, **166**, 370–392.
Foxe, J.J., Wylie, G.R., Martinez, A., Schroeder, C.E., Javitt, D.C., Guilfoyle, D., Ritter, W. & Murray, M.M. (2002) Auditory-somatosensory multisensory processing in auditory association cortex. *J. Neurophysiol.*, **88**, 540–543.
Freeman, W.J. (1988) *Nonlinear Neural Dynamics in Olfaction as a Model for Cognition. Springer Series in Brain Dynamics 1*. Springer–Verlag, Berlin, Heidelberg.
Friston, K. (2005) A theory of cortical responses. *Phil. Trans. Roy. Soc. B*, **360**, 815–836.
Friston, K.J., Harrison, L. & Penny, W. (2003) Dynamic causal modeling. *Neuroimage*, **19**, 1273–1302.
Fu, K.M., Foxe, J.J., Murray, M.M., Higgins, B.A., Javitt, D.C. & Schroeder, C.E. (2001) Attention-dependent suppression of distracter visual input can be cross-modally cued as indexed by anticipatory parieto-occipital alpha-band oscillations. *Brain Res. Cogn. Brain Res.*, **12**, 145–152.
Garrido, M.I., Kilner, J.M., Kiebel, S.J., Stephan, K.E. & Friston, K.J. (2007) Dynamic causal modelling of evoked potentials: a reproducibility study. *Neuroimage*, **36**, 571–580.
Giard, M.H. & Peronnet, F. (1999) Auditory-visual integration during multimodal object recognition in humans: a behavioral and electrophysiological study. *J. Cogn. Neurosci.*, **11**, 473–490.
Hairson, W.D., Laurienti, P.J. & Mishra, G. (2003) Multisensory enhancement of localization under conditions of induced myopia. *Exp. Brain Res.*, **152**, 404–408.
Jansen, B.H. & Rit, V.G. (1995) Electroencephalogram and visual evoked potential generation in a mathematical model of coupled cortical columns. *Biol. Cybernetics*, **73**, 357–366.
Kass, R. & Raftery, A.E. (1995) Bayes factors. *J. Am. Stat. Assoc.*, **90**, 773–795.
Kiebel, S.J., David, O. & Friston, K.J. (2006) Dynamic causal modelling of evoked responses in EEG/MEG with lead field parameterization. *Neuroimage*, **30**, May, 1273–1284.
Kiebel, S.J. & Friston, K.J. (2004) Statistical parametric mapping for event-related potentials (II): a hierarchical temporal model. *Neuroimage*, **22**, 503–520.
Kiebel, S.J., Garrido, M.I. & Friston, K.J. (2007) Dynamic causal modelling of evoked responses: the role of intrinsic connections. *Neuroimage*, **36**, 332–345.
Lakatos, P., Chen, C.M., O'Connell, M.N., Mills, A. & Schroeder, C.E. (2007) Neuronal oscillations and multisensory interaction in primary auditory cortex. *Neuron*, **53**, 279–292.
Laurienti, P.J., Perrault, T.J., Stanford, T.R., Wallace, M.T. & Stein, B.E. (2005) On the use of superadditivity as a metric for characterizing multisensory integration in functional neuroimaging studies. *Exp. Brain Res.*, **166**, 289–297.
Lopes da Silva, L., Hoek, F.H., Smits, A. & Zetterberg, L.H. (1974) Model of brain rhythmic activity: the alpha rhythm of the thalamus. *Kybernetik*, **15**, 27–37.
Macaluso, E. & Driver, J. (2005) Multisensory spatial interactions: a window onto functional integration in the human brain. *Trends Neurosci.*, **28**, 264–271.
Macaluso, E., Frith, C.D. & Driver, J. (2000) Modulation of human visual cortex by crossmodal spatial attention. *Science*, **289**, 1206–1208.
McDonald, J.J., Teder-Sälejärvi, W.A. & Hillyard, S.A. (2000) Involuntary orienting to sound improves visual perception. *Nature*, **407**, 906–908.
Mechelli, A., Price, C.J., Noppeney, U. & Friston, K.J. (2003) A dynamic causal modeling study on category effects: bottom-up or top-down mediation? *J. Cogn. Neurosci.*, **15**, 925–934.
Michel, C.M., Murray, M.M., Lantz, G., Gonzalez, S., Spinelli, L. & Grave de Peralta, R. (2004) EEG source imaging. *Clin. Neurophysiol.*, **115**, 2195–2222.
Molholm, S., Ritter, W., Javitt, D.C. & Foxe, J.J. (2004) Multisensory visual-auditory object recognition in humans: a high-density electrical mapping study. *Cereb. Cortex*, **14**, 452–465.
Molholm, S., Ritter, W., Murray, M.M., Javitt, D.C., Schroeder, C.E. & Foxe, J.J. (2002) Multisensory auditory–visual interactions during early sensory processing in humans: a high-density electrical mapping study. *Brain Res. Cogn. Brain Res.*, **14**, 115–128.
Molholm, S., Sehatpour, P., Mehta, A.D., Shpaner, M., Gomez-Ramirez, M., Ortigue, S., Dyke, J.P., Schwartz, T.H. & Foxe, J.J. (2006) Audio-visual multisensory integration in superior parietal lobule revealed by human intracanial recordings. *J. Neurophysiol.*, **96**, 721–729.
Moran, R.J., Kiebel, S.J., Stephan, K.E., Reilly, R.B., Daunizeau, J. & Friston, K.J. (2007) A neural mass model of spectral responses in electrophysiology. *NeuroImage*, **37**, 706–720.
Murray, M., Molholm, S., Michel, C.M., Heslenfeki, D.J., Ritter, W., Javitt, D.C., Schroder, C.E. & Foxe, J.J. (2005) Grabbing your ear: rapid audiotory–somatosensory multisensory interactions in low-level sensory cortices are not constrained by stimulus alignment. *Cereb. Cortex*, **15**, 963–974.
Niedermeyer, E. & Lopes da Silva, F.H. (2004) *Electroencephalography: Basic Principles, Clinical Applications and Related Fields*, 5th edn. Lippincott, Williams & Wilkins Publishing Co., USA.
Nunez, P.L. & Srinivasan, R. (2006) *Electric Fields of the Brain: The Neurophysics of EEG*. Oxford University Press, New York.
Ongur, D. & Price, J.L. (2000) The organisation of networks within the orbital and medial prefrontal cortex of rats, monkeys and humans. *Cereb. Cortex*, **10**, 206–219.
Pekkola, J., Laasonen, M., Ojanen, V., Autti, T., Jääskeläinen, I.P., Kujala, T. & Sams, M. (2006) Perception of matching and conflicting audiovisual speech in dyslexic and fluent readers: an fMRI study at 3T. *Neuroimage*, **29**, 797–807.
Penny, W.D., Stephan, K.E., Mechelli, A. & Friston, K.J. (2004) Comparing dynamic causal models. *Neuroimage*, **22**, 1157–1172.
Pleger, B., Blakenburg, F., Bestmann, S., Ruff, C.C., Wiech, K., Stephan, K.E., Friston, K.J. & Dolan, R.J. (2006) Repetitive transcranial magnetic stimulation-induces changes in sensorimotor coupling parallel improvements of somatosensation in humans. *J. Neurosci.*, **26**, 1945–1952.
Raftery, A.E. (1995) Bayesian model selection in social research. *Sociol. Methodol.*, **25**, 111–162.
Raij, T., Uutela, K. & Hari, R. (2000) Audiovisual integration of letters in the human brain. *Neuron*, **28**, 617–625.
Rao, R.P. & Ballard, D.H. (1999) Predictive coding in the visual cortex: a functional interpretation of some extra-classical receptive field effects. *Nat. Neurosci.*, **2**, 79–87.
Reep, R.L., Chandler, H.C., King, V. & Corwin, J.V. (1994) Rat posterior parietal cortex: topography of cortico-cortical thalamic connections. *Exp. Brain Res.*, **100**, 67–87.
Ross, L.A., Saint-Amour, D., Leavitt, V.M., Javitt, D.C. & Foxe, J.J. (2007) Do you see what I am saying? Exploring visual enhancement of speech comprehension in noisy environments. *Cereb. Cortex*, **17**, 1147–1153.
Saint-Amour, D., De Sanctis, P., Molholm, S., Ritter, W. & Foxe, J.J. (2007) Seeing voices: High-density electrical mapping and source-analysis of the multisensory mismatch negativity evoked during the McGurk illusion. *Neuropsychologia*, **45**, 587–597.
Schroeder, C.E. & Foxe, J.J. (2002) The timing and laminar profile of converging inputs to multisensory areas of the macaque neocortex. *Brain Res. Cogn. Brain Res.*, **14**, 187–198.
Schroeder, C.E. & Foxe, J. (2005) Contributions to low-level, 'unisensory' processing. *Curr. Opin. Neurobiol.*, **15**, 454–458.
Schroeder, C.E., Lindsley, R.W., Specht, C., Marcovici, A., Smiley, J.F. & Javitt, D.C. (2001) Somatosensory input to auditory association cortex in the macaque monkey. *J. Neurophysiol.*, **85**, 1322–1327.
Schroeder, C.E., Molholm, S., Lakatos, P., Ritter, W. & Foxe, J.J. (2004) Human-Simian correspondence in the early cortical processing of multisensory cues. *Cogn. Processing*, **5**, 140–151.
Schwartz, A.B., Cui, X.T., Weber, D.J. & Moran, D.W. (2006) Brain-controlled interfaces: review movement restoration with neural prosthetics. *Neuron*, **52**, 205–220.
Seltzer, B. & Pandya, D.N. (2004) Parietal, temporal, and occipita projections to cortex of the superior temporal sulcus in the rhesus monkey: a retrograde tracer study. *J. Comp. Neurol.*, **343**, 445–463.
Senkowski, D., Gomez-Ramirez, M., Lakatos, P., Wylie, G.R., Molholm, S., Schroeder, C.E. & Foxe, J.J. (2007) Multisensory processing and oscillatory activity: analyzing non-linear electrophysiological measures in humans and simians. *Exp. Brain Res.*, **177**, 184–195.

Steinschneider, M., Tenke, C.E., Schroeder, C.E., Javitt, D.C., Simpson, G.V., Arezzo, J.C. & Vaughan, H.G. (1992) Cellular generators of the cortical auditory evoked potential initial component. *Electroencephalogr. Clin. Neurophysiol.*, **84**, 196–200.

Stephan, K.E., Harrison, L.M., Kiebel, S.J., David, O., Penny, W.D. & Friston, K.J. (2007) Dynamic causal models of neural system dynamics: current state and future extensions. *J. Biosci.*, **32**, 129–144.

Surguladze, S.A., Calvert, G.A., Brammer, M.J., Campbell, R., Bullmore, E.T., Giampietro, V. & David, A.S. (2001) Audio-visual speech perception in schizophrenia: an fMRI study. *Psychiatry Res.*, **28**, 1–14.

Weissman, D.H., Warner, L.M. & Woldorff, M.G. (2004) The neural mechanisms for minimizing cross-modal distraction. *J. Neurosci.*, **24**, 10941–10949.

Wendling, F., Bellanger, J.J., Bartolomer, F. & Chauvel, P. (2000) Relevance of nonlinear lumped parameter models in the analysis of depth-EEG epileptic signals. *Biol. Cybernetics*, **83**, 367–378.

Wilson, H.R. & Cowan, J.D. (1973) A mathematical theory of the functional dynamics of cortical and thalamic nervous tissue. *Biol. Cybernetics*, **13**, 55–80.

Wise, S.P., Boussaoud, D., Johnson, P.B. & Caminiti, R. (1997) Premotor and parietal cortex: corticocortical connectivity and combinatorial computations. *Annu. Rev. Neurosci.*, **20**, 25–42.

Zuidpek, S., Visser, A., Bredero, M.E. & Postma, A. (2004) Multisensory integration mechanisms in haptic space perception. *Exp. Brain Res.*, **157**, 265–268.